

**MOLECULAR MECHANISMS OF MITRAGYNINE
INHIBITION ON HERG1A/1B CHANNEL**

TAY YEA LU

UNIVERSITI SAINS MALAYSIA

2018

**MOLECULAR MECHANISMS OF
MITRAGYNINE INHIBITION ON HERG1A/1B
CHANNEL**

by

TAY YEA LU

**Thesis submitted in fulfillment of the requirements
for the degree of
Doctor of Philosophy**

April 2018

ACKNOWLEDGEMENT

First and foremost, I would like to express my deepest gratitude to my supervisor, Assoc. Prof. Dr. Tan Mei Lan for her limitless dedication, continuous support, encouragement and patience in guiding me towards the completion of my Ph.D study. Over the years, I could always count on her valuable advices and feedback on my work.

In addition, I would like to express my warmest appreciation to my co-supervisors, Prof. Habibah A. Wahab and Dr. Tan Jun Jie for their time, knowledge and guidance on *in silico* and cell culture work.

I gratefully acknowledge Universiti Sains Malaysia for the financial support under USM Fellowship Scheme. This work was supported by ScienceFund from the Ministry of Science, Technology and Innovation Malaysia, and Fundamental Research Grant Scheme (FRGS) from the Ministry of Higher Education Malaysia as well as the Research University Individual Grant (RUI) from Universiti Sains Malaysia.

I would like to extend my sincere thanks to all members of the lab (Asyraf, Ee Lin, Heng Kean, Rina, Yanti, Yi Fan and Yoong Min), not only for their useful suggestions but also for all the great time, laughter and fun that we had shared.

Last but not least, my heartfelt thanks go to my family members for their unconditional love, understanding and moral support. They selflessly encouraged me to explore new directions in life and seek my own destiny. This journey would not have been possible if not for them, and I dedicate this milestone to them.

TABLE OF CONTENTS

| | |
|-----------------------|------|
| Acknowledgement | ii |
| Table of Contents | iii |
| List of Tables | x |
| List of Figures | xi |
| List of Abbreviations | xv |
| List of Symbols | xix |
| List of Units | xx |
| Abstrak | xxii |
| Abstract | xxiv |

CHAPTER 1 - INTRODUCTION

| | | |
|-------|---------------------|---|
| 1.1 | Problem statement | 1 |
| 1.2 | Objectives of study | 4 |
| 1.2.1 | General objectives | 4 |
| 1.2.2 | Specific objectives | 4 |

CHAPTER 2 - LITERATURE REVIEW

| | | |
|-------|-------------------------------|----|
| 2.1 | Mitragynine and its analogues | 6 |
| 2.2 | The cardiac action potential | 18 |
| 2.3 | Long QT syndrome (LQTS) | 22 |
| 2.3.1 | Congenital LQTS | 24 |
| 2.3.2 | Acquired LQTS | 27 |

| | | |
|----------|---|----|
| 2.4 | Regulatory perspectives | 29 |
| 2.4.1 | CPMP/986/96: Points to consider: the assessment of the potential for QT interval prolongation by non-cardiovascular medicinal products – pre-clinical studies | 29 |
| 2.4.2 | ICH S7B: Non-clinical evaluation of the potential for delayed ventricular repolarization (QT interval prolongation) by human pharmaceuticals | 29 |
| 2.5 | Human Ether-a-go-go Related Gene (HERG1) | 32 |
| 2.5.1 | Discovery of hERG1 | 32 |
| 2.5.2 | Structure of hERG1 channels | 33 |
| 2.5.3 | Biophysical characteristics of hERG1 channels | 36 |
| 2.5.4 | Structural basis of hERG1-channel gating | 42 |
| 2.5.5 | HERG1 heterogeneity: HERG1 genes and isoforms | 44 |
| 2.5.6 | Heteromeric assembly of hERG1a/1b channels | 47 |
| 2.6 | Pharmacology of hERG1 channels | 49 |
| 2.6.1 | HERG1 blockers | 49 |
| 2.6.2 | HERG1 trafficking modulators | 57 |
| 2.7 | Distribution of hERG1 channels in different tissues | 60 |
| 2.8 | Methodologies for identifying hERG1 inhibitors | 62 |
| 2.8.1 | <i>In silico</i> modeling | 62 |
| 2.8.1(a) | Ligand-based approaches | 62 |
| 2.8.1(b) | Structure-based approaches | 63 |
| 2.8.2 | <i>In vitro</i> electrophysiology | 65 |

CHAPTER 3 – MATERIALS AND METHODS

| | | |
|-----|--|----|
| 3.1 | Experimental design | 70 |
| 3.2 | Materials | 70 |
| 3.3 | Preparation of glassware and plasticware | 70 |

| | | |
|-----------|--|----|
| 3.4 | Preparation of chemical reagents | 70 |
| 3.5 | Preparation of stock and working solutions | 70 |
| 3.6 | <i>In silico</i> interaction of mitragynine and analogues with hERG1 channel | 77 |
| 3.6.1 | Preparation of macromolecule | 77 |
| 3.6.2 | Preparation of ligands | 78 |
| 3.6.3 | Grid generation and docking simulation using AutoDock 4.2 | 78 |
| 3.6.4 | Docking visualization and protein-ligand interaction prediction | 79 |
| 3.7 | Cell culture | 79 |
| 3.7.1 | Maintenance of cells in culture | 79 |
| 3.7.2 | Thawing of frozen cells | 80 |
| 3.7.3 | Subculturing of cells | 80 |
| 3.7.4 | Counting cells | 81 |
| 3.7.5 | Preserving and storing of cells | 81 |
| 3.8 | Quantification and assessment of DNA and RNA purity | 81 |
| 3.9 | Agarose gel electrophoresis | 82 |
| 3.10 | Bacterial culture | 82 |
| 3.10.1 | Preparation of Luria broth (LB) and LB agar plate | 82 |
| 3.10.2 | Transformation of competent bacterial cell | 83 |
| 3.10.3 | Purification of plasmid DNA | 83 |
| 3.11 | Molecular cloning of hERG1b | 84 |
| 3.11.1 | Establishment of pcDNA TM 3.1/Zeo(+)-hERG1b | 84 |
| 3.11.1(a) | Restriction endonuclease digestion of cDNA clone to release hERG1b | 86 |
| 3.11.1(b) | Purification of the digested hERG1b cDNA | 86 |
| 3.11.1(c) | Ligation of purified hERG1b cDNA to pcDNA TM 3.1/Zeo(+) | 87 |

| | | |
|-----------|--|-----|
| 3.11.1(d) | Amplification of the ligation mixture | 88 |
| 3.11.1(e) | PCR-screening for bacterial colonies carrying recombinant pcDNA TM 3.1/Zeo(+)-hERG1b (colony PCR) | 88 |
| 3.11.1(f) | Amplification of pcDNA TM 3.1/Zeo(+)-hERG1b | 90 |
| 3.11.2 | Verification of pcDNA TM 3.1/Zeo(+)-hERG1b | 90 |
| 3.11.2(a) | Restriction endonuclease digestion of plasmids | 90 |
| 3.11.2(b) | Sequencing | 90 |
| 3.12 | Establishment of stable HEK293-hERG1a/1b cell line | 91 |
| 3.12.1 | Stable transfection of HEK293 cell line with hERG1a | 91 |
| 3.12.2 | Stable transfection of HEK293-hERG1a with hERG1b | 91 |
| 3.12.3 | Selection of stably transfected HEK293 cell line | 92 |
| 3.12.4 | Trypan blue exclusion test | 93 |
| 3.12.5 | Verification of selected recombinant HEK293-hERG1a/1b cell line | 93 |
| 3.13 | Cell proliferation assay | 93 |
| 3.14 | One-step reverse transcription-quantitative polymerase chain reaction (RT-qPCR) | 96 |
| 3.14.1 | Isolation of total cellular RNA | 96 |
| 3.14.2 | DNase treatment of total RNA | 97 |
| 3.14.3 | Design of gene-specific primers | 97 |
| 3.14.4 | Optimization of RT-qPCR | 98 |
| 3.14.5 | Determination of RT-qPCR amplification efficiency (E) | 101 |
| 3.14.6 | Determination of relative mRNA expression of target genes | 102 |
| 3.15 | Western blotting analysis | 102 |
| 3.15.1 | Isolation of total protein | 102 |

| | | |
|--------|--|-----|
| 3.15.2 | Determination of protein concentration using Bio-Rad DC™ protein assay | 104 |
| 3.15.3 | Sodium dodecyl sulfate polyacrylamide gel electrophoresis (SDS-PAGE) | 104 |
| 3.15.4 | Immunoblotting and visualizing of proteins | 106 |
| 3.16 | Electrophysiology | 110 |
| 3.16.1 | Preparation of electrophysiology solutions | 112 |
| 3.16.2 | Cell culture for electrophysiology | 112 |
| 3.16.3 | Cell harvesting | 112 |
| 3.16.4 | Recording hERG1a/1b current | 113 |
| 3.17 | Immunofluorescence analysis | 116 |
| 3.17.1 | Coating of glass cover slips for growing cells | 116 |
| 3.17.2 | Fixation and permeabilization of cells | 118 |
| 3.17.3 | Immunofluorescence staining and visualization | 118 |
| 3.18 | Co-immunoprecipitation | 119 |
| 3.18.1 | Total protein extraction for co-immunoprecipitation | 119 |
| 3.18.2 | Co-immunoprecipitation | 121 |
| 3.19 | Treatment of HEK293-hERG1a/1b cells | 124 |
| 3.19.1 | Treatment of HEK293-hERG1a/1b cells to determine the effects of mitragynine on hERG1a/1b mRNA and protein expression | 124 |
| 3.19.2 | Treatment of HEK293-hERG1a/1b cells to determine the effects of mitragynine on hERG1a/1b protein expression using immunofluorescence visualization | 125 |
| 3.19.3 | Treatment of HEK293-hERG1a/1b cells to determine the effects of mitragynine on interactions between hERG1a and cytosolic chaperones, Hsp70 and Hsp90 | 126 |
| 3.20 | Data analysis | 126 |

CHAPTER 4 – RESULTS

| | | |
|----------|---|-----|
| 4.1 | <i>In silico</i> interactions of mitragynine and analogues with hERG1 channel | 127 |
| 4.2 | Establishment of pcDNA [™] 3.1/Zeo(+)-hERG1b | 137 |
| 4.3 | Establishment of stable HEK293-hERG1a/1b cell line | 139 |
| 4.3.1 | Selection of stably transfected HEK293 cell line | 139 |
| 4.3.2 | The effect of transfection on cell viability using trypan blue exclusion test | 142 |
| 4.4 | Verification of selected recombinant HEK293-hERG1a/1b cell line | 144 |
| 4.4.1 | Verification of mRNA expression of hERG1a/1b in HEK293 cell line using RT-qPCR analysis | 144 |
| 4.4.1(a) | Purity and integrity of isolated total RNA | 144 |
| 4.4.1(b) | Optimization of RT-qPCR analysis | 144 |
| 4.4.1(c) | Verification of hERG1a and hERG1b mRNA expression in the HEK293 cell line | 149 |
| 4.4.2 | Verification of protein expression of hERG1a/1b in HEK293 cell line | 152 |
| 4.4.3 | Verification of hERG1a/1b current using whole cell planar patch clamp analysis | 152 |
| 4.5 | Cell proliferation assay | 159 |
| 4.6 | Effects of mitragynine on hERG1a/1b current | 161 |
| 4.7 | Effects of mitragynine on hERG1a/1b mRNA expression | 165 |
| 4.8 | Effects of mitragynine on hERG1a/1b protein expression | 165 |
| 4.8.1 | Western blotting | 165 |
| 4.8.2 | Immunofluorescence | 170 |
| 4.9 | Effects of mitragynine on hERG1-cytosolic chaperones interaction | 173 |
| 4.9.1 | Expression of endogenous Hsp70 and Hsp90 in HEK-hERG1a/1b cells | 173 |

| | | |
|-------|---|-----|
| 4.9.2 | Effects of mitragynine on hERG1a/Hsp70 and hERG1a/Hsp90 complexes | 174 |
|-------|---|-----|

CHAPTER 5 – DISCUSSION

| | | |
|-----|--|-----|
| 5.1 | General discussion | 181 |
| 5.2 | <i>In silico</i> interaction of mitragynine and analogues with hERG1 channel | 185 |
| 5.3 | Development of whole-cell patch-clamp assay using a recombinant HEK293 cell line expressing hERG1a/1b channel | 189 |
| 5.4 | Effects of mitragynine on hERG1a/1b current | 195 |
| 5.5 | Effects of mitragynine on hERG1a/1b mRNA and protein expression, as well as the interactions between hERG1a protein and cytosolic chaperones (Hsp70 and Hsp90) | 198 |
| 5.6 | Limitation of present studies and future direction | 204 |

CHAPTER 6 – CONCLUSION

206

REFERENCES

207

APPENDICES

LIST OF PUBLICATIONS AND PROCEEDINGS

LIST OF TABLES

| | | Page |
|-------------------|---|-------------|
| Table 2.1 | Alkaloid profile of <i>Mitragyna speciosa</i> Korth | 8 |
| Table 2.2 | Summary of the genes and encoded proteins in subtypes of the congenital long QT syndrome | 26 |
| Table 2.3 | List of common drugs known to inhibit hERG1 channels leading to QT prolongation and TdP, and their inhibition mechanisms | 50 |
| Table 3.1 | Materials and reagents used with their manufacturers | 72 |
| Table 3.2 | Stock solution of chemical reagents and their composition | 74 |
| Table 3.3 | Stock and working solutions and their composition | 75 |
| Table 3.4 | Nucleotide sequences of primers for the validation of recombinant plasmids using colony PCR | 89 |
| Table 3.5 | RT-qPCR reaction mix composition | 99 |
| Table 3.6 | RT-qPCR amplification protocol | 100 |
| Table 3.7 | Composition of resolving (separating) gel and stacking (upper) gel for SDS-PAGE | 105 |
| Table 3.8 | The optimized dilution solutions for each antibody used for Western blotting, immunofluorescence and co-immunoprecipitation | 108 |
| Table 3.9 | Voltage-clamp protocols used to characterize hERG1a/1b current | 115 |
| Table 3.10 | Compounds used for patch-clamp assay | 117 |
| Table 4.1 | A summary of the molecular interactions of compounds within the inner cavity of the pore domains of hERG1 | 129 |
| Table 4.2 | Nucleotide sequences, optimum annealing temperature and RT-qPCR efficiency of primers | 146 |

LIST OF FIGURES

| | | Page |
|--------------------|---|-------------|
| Figure 2.1 | The electrical activity of the heart presented on the surface cardiac electrocardiogram (ECG) | 19 |
| Figure 2.2 | The ventricular cardiac action potential and cardiac ion channels | 20 |
| Figure 2.3 | Relationship between delayed repolarization, prolonged QT interval and Torsade de Pointes (TdP) cardiac-arrhythmia | 23 |
| Figure 2.4 | Non-clinical testing strategy on cardiotoxicity assessment (ICH S7B guideline) | 31 |
| Figure 2.5 | Phylogenetic tree for the voltage-gated K ⁺ channel superfamily | 34 |
| Figure 2.6 | Structural features for hERG1 channel | 35 |
| Figure 2.7 | Gating of the hERG1 channels | 38 |
| Figure 2.8 | Electrophysiological properties of hERG1 current | 40 |
| Figure 2.9 | Protein structure of hERG1 isoforms | 45 |
| Figure 2.10 | Putative drug-binding site for hERG1 and EAG1 | 54 |
| Figure 2.11 | Biogenesis of hERG1 channels | 58 |
| Figure 2.12 | A typical docking workflow of molecular docking | 66 |
| Figure 2.13 | The schematic set up of patch clamp experiments | 68 |
| Figure 3.1 | Overall flow chart showing steps in the experimental design to elucidate the molecular mechanism of mitragynine on hERG1a/1b channel | 71 |
| Figure 3.2 | Maps of the plasmids pCMV6-Neo-hERG1a, pCMV6-XL4-hERG1b and pcDNA TM 3.1/Zeo(+)-hERG1b, used in the establishment of stable HEK293-hERG1a/1b cell line | 85 |
| Figure 3.3 | Calculation for the percentage of growth using the cell proliferation assay | 95 |
| Figure 3.4 | Relative quantification of a single target gene in the presence of one or more reference genes in each sample | 103 |
| Figure 3.5 | The Port-a-Patch electrophysiology workstation | 111 |

| | | |
|--------------------|--|-----|
| Figure 3.6 | The 15 spots on the slide for image capturing and image selection for hERG1a and hERG1b protein expression using ImageJ software | 120 |
| Figure 3.7 | The experimental workflow to determine the effects of mitragynine on the interactions between hERG1a and cytosolic chaperones, Hsp70 and Hsp90 | 122 |
| Figure 3.8 | A simplified diagram of co-immunoprecipitation (Co-IP) reaction | 123 |
| Figure 4.1 | A representative of cluster analysis of docking result | 128 |
| Figure 4.2A | Molecular interaction of mitragynine within the inner cavity of the pore domain of hERG1 channel | 131 |
| Figure 4.2B | Molecular interaction of paynantheine within the inner cavity of the pore domain of hERG1 channel | 132 |
| Figure 4.2C | Molecular interaction of speciogynine within the inner cavity of the pore domain of hERG1 channel | 133 |
| Figure 4.2D | Molecular interaction of speciociliatine within the inner cavity of the pore domain of hERG1 channel | 134 |
| Figure 4.2E | Molecular interaction of terfenadine within the inner cavity of the pore domain of hERG1 channel | 135 |
| Figure 4.2F | Molecular interaction of pentamidine within the inner cavity of the pore domain of hERG1 channel | 136 |
| Figure 4.3 | Agarose gel electrophoresis images | 138 |
| Figure 4.4 | Comparison between the sequence of the insert in purified pcDNA TM 3.1/Zeo(+)-hERG1b against sequence in GenBank | 140 |
| Figure 4.5 | Images of transfected cells after growing in complete DMEM supplemented with 500 µg/ml Geneticin [®] and 300 µg/ml Zeocin TM | 141 |
| Figure 4.6 | The effects of transfection on the viability of HEK293 and HEK293-hERG1a/1b cells | 143 |
| Figure 4.7 | A representative image of the purity and integrity of total RNA isolated from HEK293-hERG1a/1b cells | 145 |
| Figure 4.8 | Optimization of RT-qPCR primer pair for hERG1a | 147 |
| Figure 4.9 | Optimization of RT-qPCR primer pair for hERG1b | 148 |

| | | |
|--------------------|--|-----|
| Figure 4.10 | Standard curve plots for amplification efficiency of hERG1a, hERG1b, ACTB and GAPDH gene | 150 |
| Figure 4.11 | Representative RT-qPCR amplification curve for hERG1a and hERG1b for stably transfected HEK293-hERG1a/1b and untransfected HEK293 cells, and fold change of hERG1a and hERG1b mRNA expression in HEK293-hERG1a/1b cells relative to HEK293 | 151 |
| Figure 4.12 | Western blot analysis for the hERG1a (155 kDa and 135 kDa) and hERG1b (95 kDa and 80 kDa) protein expression in HEK293-hERG1a/1b cells and optimization of the amount of total protein used in immunodetection | 153 |
| Figure 4.13 | Electrophysiological properties of hERG1a/1b current in HEK293-hERG1a/1b cells | 154 |
| Figure 4.14 | The fully activated I-V relation of hERG1a/1b current | 156 |
| Figure 4.15 | Inactivation and recovery from inactivation of hERG1a/1b current in HEK293-hERG1a/1b cells | 157 |
| Figure 4.16 | The effects of mitragynine on HEK293 and HEK293-hERG1a/1b cell proliferation | 160 |
| Figure 4.17 | Representative hERG1a/1b tail current traces before and after application of sertindole, terfenadine, propafenone and fluoxetine at room temperature | 162 |
| Figure 4.18 | The effects of mitragynine on hERG1a/1b tail currents. | 163 |
| Figure 4.19 | Concentration dependent block of hERG1a/1b current by sertindole, terfenadine, propafenone, fluoxetine and mitragynine | 164 |
| Figure 4.20 | The effects of arsenic trioxide and mitragynine on mRNA expression of hERG1a and hERG1b | 166 |
| Figure 4.21 | The effects of arsenic trioxide on the hERG1a/1b protein expression | 167 |
| Figure 4.22 | The effects of mitragynine on the hERG1a/1b protein expression | 168 |
| Figure 4.23 | Immunofluorescence illustrating hERG1a protein on the HEK293-hERG1a/1b cells treated by 0.1% (v/v) DMSO, 1 μ M As ₂ O ₃ , 1 μ M mitragynine and 10 μ M mitragynine | 171 |
| Figure 4.24 | Immunofluorescence illustrating hERG1b protein on the HEK293-hERG1a/1b cells treated by 0.1% (v/v) DMSO, 1 μ M As ₂ O ₃ , 1 μ M mitragynine and 10 μ M mitragynine | 172 |

| | | |
|--------------------|---|-----|
| Figure 4.25 | The effects of arsenic trioxide on the expression levels of endogenous Hsp70 and Hsp90 | 175 |
| Figure 4.26 | The effects of mitragynine on the expression levels of endogenous Hsp70 and Hsp90 | 176 |
| Figure 4.27 | The effects of arsenic trioxide (As ₂ O ₃) and mitragynine on the interaction between cg-hERG1a (135 kDa) with Hsp70 | 177 |
| Figure 4.28 | The effects of As ₂ O ₃ and mitragynine on the interaction between cg-hERG1a (135 kDa) with Hsp90 | 179 |
| Figure 5.1 | A simplified diagram illustrating the possible molecular mechanisms for mitragynine inhibition on hERG1a/1b channels | 203 |

LIST OF ABBREVIATIONS

| | |
|----------------------|--|
| τ_{fast} | Fast time constant |
| 2D | Two-dimensional |
| A ₂₃₀ | Absorbance at 230 nm |
| A ₂₆₀ | Absorbance at 260 nm |
| A ₂₈₀ | Absorbance at 280 nm |
| ACTB | Beta-actin |
| ANOVA | Analysis of variance |
| APS | Ammonium persulfate |
| BSA | Bovine serum albumin |
| CaCl ₂ | Calcium chloride |
| cDNA | Complementary deoxyribonucleic acid |
| cg | Core-glycosylated |
| CO ₂ | Carbon dioxide |
| COPII | Coat protein complex II |
| C _q | Quantification cycle |
| DAPI | 4',6-diamidino-2-phenylindole dihydrochloride |
| DI H ₂ O | Deionized water |
| DMEM | Dulbecco's Modified Eagle Medium |
| DMSO | Dimethyl sulfoxide |
| DNA | Deoxyribonucleic acid |
| dNTP | Deoxynucleotide |
| DSP | Dithiobis(succinimidylpropionate) |
| E | Efficiency |
| ECL | Enhanced chemiluminescence |
| EGTA | Ethylene-bis(oxyethylenitrilo)tetraacetic acid |

| | |
|-------------------|--|
| <i>exp</i> | Exponential |
| FBS | Fetal bovine serum |
| FEB | Free energy of binding |
| fg | Fully-glycosylated |
| FP | Forward primer |
| GAPDH | Glyceraldehyde-3-phosphate dehydrogenase |
| GI ₅₀ | Half maximal growth inhibitory concentration |
| <i>h</i> | Hill coefficient |
| HCl | Hydrochloric acid |
| HEK293 | Human embryonic kidney 293 |
| HEPES | 4-(2-hydroxyethyl)-1-piperazineethanesulfonic acid |
| hERG1 | Human ether-a-go-go related gene 1 |
| HRP | Horseradish peroxidase |
| Hsp | Heat shocked protein |
| IC ₅₀ | Half maximal inhibitory concentration |
| IgG | Immunoglobulin G |
| I _{max} | Maximum peak tail current |
| I _{tail} | Peak tail current |
| I-V | Current-voltage |
| <i>k</i> | Slope factor |
| KCl | Potassium chloride |
| K-Fluoride | Potassium fluoride |
| K _i | Estimated inhibition constant |
| KOH | Potassium hydroxide |
| LB | Luria broth |
| LC ₅₀ | Half maximal lethal concentration |
| MEM | Minimum Essential Medium |

| | |
|-------------------|--|
| MgCl ₂ | Magnesium chloride |
| mRNA | Messenger ribonucleic acid |
| Na ⁺ | Sodium ion |
| NaCl | Sodium chloride |
| NaOH | Sodium hydroxide |
| <i>p</i> | Probability |
| PBS | Phosphate buffered saline |
| PBST | 0.1% (v/v) Tween-20-phosphate buffered saline |
| PCR | Polymerase chain reaction |
| PDB | Protein Data Bank |
| PG | Percentage growth |
| PMSF | Phenylmethylsulfonyl fluoride |
| PVDF | Polyvinylidene fluoride |
| QSAR | Quantitative structure-activity relationship |
| R ² | Coefficient of determination |
| RIPA | Radioimmunoprecipitation assay |
| RMSD | Root-mean-square deviation |
| RNA | Ribonucleic acid |
| RP | Reverse primer |
| rRNA | Ribosomal ribonucleic acid |
| RT-qPCR | Reverse transcription-quantitative polymerase chain reaction |
| SDS | Sodium dodecyl sulfate |
| SDS-PAGE | Sodium dodecyl sulfate polyacrylamide gel electrophoresis |
| SEM | Standard error of the mean |
| TBE | Tris/Borate/EDTA |
| TE | Tris/EDTA |
| TEMED | Tetramethylethylenediamine |

| | |
|-------------------|-----------------------------------|
| TGI | Total growth inhibition |
| t_{zero} | Time zero |
| UV | Ultraviolet |
| v/v | Volume per volume |
| $V_{1/2}$ | Half maximal activation potential |
| w/v | Weight per volume |

LIST OF SYMBOLS

| | |
|-------------------------------|--------------------------|
| \sim | Approximately |
| $*$ | Asterisk |
| β | Beta |
| $>$ | Greater than |
| \geq | Greater than or equal to |
| $<$ | Less than |
| \leq | Less than or equal to |
| π | Pi |
| \pm | Plus or minus |
| $\text{\textcircled{R}}$ | Registered trademark |
| τ | Tau |
| TM | Trademark |

LIST OF UNITS

| | |
|-----------------|--------------------------|
| % | Percentage |
| °C | Degree Celsius |
| μg | Microgram |
| μg/ml | Microgram per milliliter |
| μl | Microliter |
| μm | Micrometer |
| μM | Micromole |
| A | Ampere |
| Å | Ångström |
| cells/ml | Cells per milliliter |
| cm | Centimeter |
| cm ² | Square centimeter |
| G | Gram |
| GΩ | Giga Ohm |
| h | Hour |
| kb | Kilobase pair |
| kPa | Kilopascal |
| M | Mole |
| mg | Milligram |
| min | Minute |
| ml | Milliliter |
| mm | Millimeter |
| mM | Millimole |
| mOsmol | Milliosmole |
| ms | Millisecond |

| | |
|-------|-------------------------|
| mV | Millivolt |
| MΩ | Mega Ohm |
| N | Normal |
| ng | Nanogram |
| ng/μl | Nanogram per microliter |
| nm | Nanometer |
| nM | Nanomole |
| rpm | Revolutions per minute |
| s | Second |
| U/μl | Unit per microliter |
| V | Volt |
| x g | Times gravity |

MEKANISME MOLEKULAR MITRAGYNINE ATAS PERENCATAN SALURAN HERG1A/1B

ABSTRAK

Daun *Mitragyna speciosa* Korth (*M. speciosa*), pada umumnya dikenali sebagai daun ketum di Malaysia, telah digunakan secara meluas untuk merawat penyakit yang lazim seperti jangkitan usus, sakit otot, batuk, cirit-birit, kencing manis, darah tinggi dan untuk memperbaiki peredaran darah. Walau bagaimanapun, keadaan keselamatan dan potensi penyalahgunaan tumbuhan ini yang mempamerkan kesan ketagihan semakin membimbangkan. Profil keselamatan tumbuhan ini tidak dijelaskan sepenuhnya. *Ether-a-go-go-related* gen manusia 1 (hERG1) mengkod subunit yang mendasari pembentukan liang protein saluran lambat kalium (I_{Kr}). Sekatan farmakologi atas I_{Kr} boleh menyebabkan sindrom perolehan QT panjang yang bakal mengakibatkan aritmia jantung yang boleh membawa maut. Justeru, kajian ini bertujuan untuk menyelidik kesan mitragynine, sebatian bioaktif utama dalam ekstrak daun ketum, atas perencatan saluran hERG1a/1b dengan menggunakan kaedah *in silico* dan *in vitro*. Simulasi dok telah dijalankan dengan menggunakan model homologi hERG1 dan interaksi serta affiniti pengikatan antara molekul telah dianalisis. Sel rekombinan HEK293-hERG1a/1b telah dihasilkan untuk menilai kesan mitragynine atas arus dan ungkapan mRNA hERG1a/1b masing-masing dengan menggunakan analisis sistem patch-clamp seluruh sel dan RT-qPCR. Di samping itu, ungkapan protein saluran hERG1a/1b telah dikaji dengan menggunakan analisis Western blot dan imuno pendarfluor. Simulasi dok mencadangkan mitragynine berkemungkinan merupakan perencat hERG1 dengan membentuk interaksi π dengan

asid amino yang penting bagi saluran hERG1, yaitu Tyr652 and Phe656. Sistem patch-clamp seluruh sel yang menggunakan sel rekombinan HEK293-hERG1a/1b telah berjaya dihasilkan dan disahkan dengan beberapa penyekat hERG1 yang diketahui. Sertindole, terfenadine, propafenone dan fluoxetine masing-masing mendedahkan nilai IC_{50} 17.44 nM ($h = 0.76$), 66.44 nM ($h = 0.84$), 361.8 nM ($h = 1.56$) dan 640.5 nM ($h = 1.19$). Mitragynine didapati menyekat arus hERG1a/1b dengan IC_{50} 332.7 nM ($h = 0.61$). Namun, mitragynine tidak menunjukkan kesan penyekatan yang nyata atas ungkapan mRNA hERG1a/1b ($p > 0.05$). Di samping itu, ungkapan protein hERG1a/1b tidak terjejas pada kepekatan yang rendah ($p > 0.05$). Sebaliknya, analisis Western blot dan imuno pendarfluor menunjukkan pengurangan yang nyata dalam ungkapan protein hERG1a pada 10 μ M ($p = 0.0217$ dan 0.0028). Akan tetapi, ungkapan protein hERG1b tidak terjejas ($p = 0.4677$ dan 0.2667). Analisis Western blot telah menunjukkan peningkatan yang nyata dalam ungkapan protein hERG1a yang tidak berglikolisis penuh (cg-hERG1a) ($p = 0.0188$), dan pengurangan yang nyata dalam ungkapan protein hERG1a yang berglikolisis penuh (fg-hERG1a) ($p = 0.0217$). Pemerhatian ini mencadangkan aliran trafik hERG1a telah terjejas. Namun, mitragynine tidak menyekat interaksi antara cg-hERG1a dengan chaperone sitoplasma, Hsp70 dan Hsp90. Sebaliknya, mitragynine meningkatkan interaksi antara cg-hERG1a dengan Hsp90 ($p = 0.0101$). Pemerhatian ini mencadangkan bahawa mitragynine menyekat aliran trafik hERG1a dengan menggunakan mekanisme yang lain. Kesimpulannya, mitragynine merencat arus hERG1a/1b dengan penyekatan terus saluran hERG1a/1b pada kepekatan yang rendah serta pengurangan ungkapan protein hERG1a/1b pada kepekatan yang tinggi. Kajian ini mencadangkan alkaloid ini berkemungkinan menyebabkan ketoksikan terhadap jantung.

MOLECULAR MECHANISMS OF MITRAGYNINE INHIBITION ON HERG1A/1B CHANNEL

ABSTRACT

The leaves of *Mitragyna speciosa* Korth (*M. speciosa*), commonly known as ketum in Malaysia, have been widely used to treat common illnesses such as intestinal infections, muscle pain, cough, diarrhea, diabetes, hypertension and to improve blood circulation. Nevertheless, there are growing concerns about the safety and abuse or misuse potentials of the plant which exhibits addictive effects. The safety profile of the plant is not fully elucidated. The *human ether-a-go-go-related gene 1* (hERG1) encodes the pore-forming subunit underlying cardiac rapidly delayed rectifier potassium current (I_{Kr}). Pharmacological blockade of the I_{Kr} can cause acquired long QT syndrome, which may lead to lethal cardiac arrhythmias. Hence, this study aims to investigate the effects of mitragynine, the major bioactive compound derived from the leave extracts of ketum, on hERG1a/1b channel inhibition, using both *in silico* and *in vitro* approaches. Docking simulations were performed using a hERG1 homology model and their molecular interactions and binding affinities were analyzed. A recombinant HEK293-hERG1a/1b cell line was established and subsequently used to evaluate the effects of mitragynine on hERG1a/1b current and mRNA expression using whole cell patch clamp and RT-qPCR analyses respectively. In addition, the protein expression of hERG1a/1b channels was studied using both Western blot and immunofluorescence analyses. *In silico* study shows that mitragynine is likely a hERG1 inhibitor by forming π interactions with the important residues, Tyr652 and Phe656, of the hERG1 channel. Whole cell patch clamp system using the recombinant

HEK293-hERG1a/1b cell line was successfully established and verified using several known hERG1 blockers. Sertindole, terfenadine, propafenone and fluoxetine revealed IC₅₀ values of 17.44 nM ($h = 0.76$), 66.44 nM ($h = 0.84$), 361.8 nM ($h = 1.56$) and 640.5 nM ($h = 1.19$) respectively. On the other hand, mitragynine was found to inhibit the current with an IC₅₀ of 332.7 nM ($h = 0.61$). However, mitragynine did not show significant inhibitory effect ($p > 0.05$) on the hERG1a/1b mRNA expression. At lower concentration, the hERG1a/1b protein expression was not affected ($p > 0.05$). Interestingly, Western blot and immunofluorescence analyses showed a significant reduction in the hERG1a protein expression at 10 μ M ($p = 0.0217$ and 0.0028 respectively), but not hERG1b ($p = 0.4677$ and 0.2667 respectively). Western blot analysis showed an increase in protein expression of core-glycosylated (cg) hERG1a ($p = 0.0188$) but a reduction in expression of fully-glycosylated (fg) hERG1a ($p = 0.0217$), suggesting an impaired hERG1a trafficking. Nevertheless, mitragynine did not inhibit the interactions between cg-hERG1a and cytosolic chaperones, Hsp70 and Hsp90. On the other hand, mitragynine treated cells have up-regulated the hERG1a-Hsp90 complexes ($p = 0.0101$), indicating a different trafficking inhibition pathway by mitragynine. In conclusion, mitragynine inhibits hERG1a/1b current by direct channel blockade at lower concentration and reduces hERG1a/1b channel protein expression at higher concentration, suggesting the possibility of the alkaloid to cause cardiac toxicity.

CHAPTER 1

INTRODUCTION

1.1 Problem statement

In recent years, there has been an increased demand for herbal medicines all over the world, including Malaysia. According to World Health Organization (WHO), herbal medicines consist of herbs, herbal materials, herbal preparations and finished herbal products, which contain parts of plants, other plant materials, or combinations, as active ingredients (WHO, 2017). Herbal medicines are widely used by the public for general health care, for the prevention or treatment of minor ailments, as well as for chronic illnesses (Aziz and Tey, 2009; Sofowora *et al.*, 2013).

A survey conducted in 2009 indicated that 88.9% and 87.3% of the Malaysian population utilized biologically-based remedy such as supplements, vitamins and herbs for health problem and health maintenance respectively (Siti *et al.*, 2009). One of the key reasons for the public to rely on herbal medicines is that these products are relatively inexpensive. In addition, majority of the public believe that herbal medicines do not contain harmful chemicals and are free of side effects comparing to commercially available pharmaceutical drugs (Law and Soon, 2013). This is not always true, especially when herbs are consumed with prescription drugs, over-the-counter medications, or other herbs, in which drug-herb interactions are very commonly reported (Wachtel-Galor and Benzie, 2011; Singh and Zhao, 2017).

The widespread use of herbal medicines by the Malaysian population is of special concern, particularly when herbal medicines are not strictly controlled by the Malaysian Drug Control Authority (DCA). The safety and quality assessment of herbal medicines by the DCA is restricted to regulation on the content of specified

contaminants and adulterants such as microorganisms and heavy metals (Aziz and Tey, 2009; Chandra Siri *et al.*, 2013). Lack of knowledge and scientific evidence on the safety of herbal medicines may pose additional risk to the public.

Mitragyna speciosa Korth from the Rubiaceae (coffee) family is a medicinal plant which is native to countries in South-East Asia, especially in Thailand, Malaysia, Indonesia and Papua New Guinea. It is commonly known as “ketum” or “Biak-Biak” in Malaysia or “kratom” in Thailand (Ahmad and Aziz, 2012; Hassan *et al.*, 2013). In Malaysia, the plant is predominantly found in the northern states, especially Perlis and Kedah, and it is commonly sold as beverages and teas (Vicknasingam *et al.*, 2010; Ahmad and Aziz, 2012). Ketum leaves have been used by natives to treat common illnesses, for instance, intestinal infections, cough, diarrhea, muscle pain, diabetes and hypertension, as well as to improve blood circulation (Adkins *et al.*, 2011; Ahmad and Aziz, 2012; Hassan *et al.*, 2013). Moreover, the leaves are popular for their energizing and pain alleviating effects that are known to possess psychostimulant- and addictive-like properties, depending on the dosage taken (Singh *et al.*, 2014).

Apart from traditional uses, ketum is often misused for recreational purposes. A survey conducted in two northern states of Malaysia (Kedah and Penang) revealed that 90% of the subjects relied on ketum as an inexpensive alternative to the more expensive opiates, and 84% used it to alleviate their opioid withdrawal symptoms (Vicknasingam *et al.*, 2010). Another recent study indicated that more than half of the regular ketum users developed severe ketum dependence problems, whereas 45% showed a moderate ketum dependence (Singh *et al.*, 2014).

Usage of ketum is no longer restricted to its native country. In recent years, ketum containing preparations, which are in the form of dried leaf, resin or crude

extracts, are widely accessible on the internet and users can conveniently buy them online (Schmidt *et al.*, 2011; Cinosi *et al.*, 2015). Ketum is generally consumed deliberately to gain the desirable effects of euphoria, to manage opiate withdrawal, or to ease chronic pain. Most users prefer self-treat to avoid the stigma of being classified as drug-dependent (Ramanathan and Mansor, 2014). Several poisoning and fatal cases related to ketum and mitragynine (the main alkaloid in the leave extracts of ketum) have been reported. However, the underlying causes remain ambiguous (Boyer *et al.*, 2008; Nelsen *et al.*, 2010; Kronstrand *et al.*, 2011; Neerman *et al.*, 2013).

Cardiac toxicity is one of the major reasons responsible for the suspension of preclinical or clinical drug discovery programs, for severe adverse drug reactions, and for withdrawal of licensed drugs (Schramm *et al.*, 2014). Between 1957 and 2007, there were 47 cases of post-marketing withdrawal of drugs, in which 45% of these were due to concerns about cardiac toxicity (Redfern *et al.*, 2010). Likewise, 27% of the potential new drug molecules failed in the pre-clinical stage since 1990s due to cardiac toxicity (Turner *et al.*, 2014). The risk of developing Torsade de Pointes (TdP), a lethal cardiac arrhythmia which is portrayed by long QT interval in electrocardiogram, has been the main reason for the removal of approximately 26% of post-marketed drugs between 1990 and 2005 (Valentin, 2010; Kothari *et al.*, 2015).

The human ether-a-go-go related gene (hERG1) channel is the currently most important target for cardiac safety evaluation (Gintant *et al.*, 2016; Grandi *et al.*, 2017). Inhibition of hERG1 by a wide range of drug molecules can prolong repolarization of the cardiac action potential and eventually lead to serious complication, such as TdP and sudden cardiac death (Kallergis *et al.*, 2012). To reduce cardiac risks following drug development, both the pharmaceutical industry and U.S. Food and Drug Administration (FDA) have mandated *in vitro* cardiac toxicity screening early in new

chemical entity (NCE) development (FDA, 2005a; Liang *et al.*, 2013). Nevertheless, little is known about the hERG1 inhibitory potential of herbal medicines (Schramm *et al.*, 2014). To date, several natural compounds under the class of flavonoids (e.g., acacetin and naringenin) and alkaloids (e.g., changrolin, dauricine, and lobeline) are known as hERG1 blockers *in vitro* (Zitron *et al.*, 2005; Schramm *et al.*, 2014; De Mieri *et al.*, 2015). Furthermore, it was revealed that drinking 1 L of pink grapefruit juice, which contains large amounts of naringenin, led to significant QT prolongation in healthy volunteers (Zitron *et al.*, 2005). However, the cardiac toxicity of ketum or mitragynine is poorly understood. Hence, there is a vital need to evaluate comprehensively the potential risks of ketum or mitragynine in hERG1 channel inhibition.

1.2 Objectives of study

1.2.1 General objective

The general objective of the present work is to determine the molecular mechanism of mitragynine inhibition on the hERG1a/1b channel.

1.2.2 Specific objectives

The specific objectives of the present work are:

1. To predict interaction of hERG1 with mitragynine and its analogues using an *in silico* approach.
2. To develop a whole-cell patch-clamp assay using a recombinant HEK293 cell line expressing human ether-a-go-go related gene 1a/1b (hERG1a/1b) channel.
3. To determine the effects of mitragynine on hERG1a/1b current.

4. To determine the effects of mitragynine on hERG1a/1b mRNA and protein expression.
5. To determine the effects of mitragynine on the interactions between hERG1a protein and cytosolic chaperones Hsp70 and Hsp90.

CHAPTER 2

LITERATURE REVIEW

2.1 Mitragynine and its analogues

Mitragynine is a major bioactive compound isolated from the leave extracts of *Mitragyna speciosa* Korth, which is commonly known as “ketum” in Malaysia. The plant is a tall leafy plant which can grow to a normal height of 4 – 9 m and 5 m wide and it grows mainly in tropical and sub-tropical regions of South-East Asia and Africa. (Hassan *et al.*, 2013). The leaves of the plant are either made into drink, chewed when freshly picked, or smoked when dried (Ahmad and Aziz, 2012).

Ketum is well-known for its addictive properties. The usage of ketum in Malaya (Peninsula Malaysia in olden days) was first reported by Burkill in 1935 as a wound poultice, remedy for fever and an alternative for opium (Burkill, 1935; Ahmad and Aziz, 2012). Traditionally, ketum has been used by the natives to disengage addicts from heroin addiction, to cure diarrhea, to treat diabetes as well as to improve blood circulation (Chan *et al.*, 2005; Singh *et al.*, 2017). In addition, the leaves of the plant have long been consumed by male manual laborers to enhance physical endurance and as a means to overcome stress (Vicknasingam *et al.*, 2010; Singh *et al.*, 2016). Opiate addicts rely on ketum to reduce consumption of more expensive opiates, to alleviate opium withdrawal symptoms and to treat chronic pain (Boyer *et al.*, 2008; Vicknasingam *et al.*, 2010; Cinosi *et al.*, 2015). Nevertheless, long-term consumption of ketum can lead to misuse, abuse, dependence and addiction (Boyer *et al.*, 2008; Trakulsrichai *et al.*, 2013; Galbis-Reig, 2016). Typical withdrawal symptoms reported include aggression, hostility, excessive tearing, inability to work and jerky movements of limbs, whereas long-term usage of ketum has been known to cause symptoms such as insomnia, anorexia and weight loss (Suwanlert, 1975; Ahmad and Aziz, 2012).

Extensive phytochemical studies carried out since the 1960s have revealed the natural occurrence of alkaloids, terpenoids and flavonoids in the plant material of the genus *Mitragyna* (Brown *et al.*, 2017). The major phytochemicals isolated and characterized from the plant *M. speciosa* (ketum) are the alkaloid compounds (summarized in Table 2.1) (Beckett *et al.*, 1966a; Beckett *et al.*, 1966b; Shellard *et al.*, 1978a; Shellard *et al.*, 1978b; Houghton and Said, 1986; Houghton *et al.*, 1991; Takayama *et al.*, 1998; Takayama *et al.*, 1999; Takayama *et al.*, 2000; Takayama, 2004; Kitajima *et al.*, 2006; Hassan *et al.*, 2013; Ali *et al.*, 2014; Brown *et al.*, 2017). The main pharmacologically active alkaloids derived from the ketum leaves are the indole alkaloids, mitragynine and 7-hydroxymitragynine (7-HMG) (Warner *et al.*, 2016). Mitragynine, accounting for approximately 12-66% of the total alkaloid mixture, appears to be the dominant active alkaloid and is exclusive to the plant whereas 7-HMG accounts for only up to 2% (Hassan *et al.*, 2013; Warner *et al.*, 2016).

The alkaloid content varies depending on stage of maturity or ecotype of the plant (Shellard *et al.*, 1978b; Takayama *et al.*, 1998; Leon *et al.*, 2009; Brown *et al.*, 2017). Depending on ecotype, mitragynine makes up approximately 66% of the total alkaloid content in plants of Thai origin, whereas it constitutes only 12% in plants of Malaysian origin (Ponglux *et al.*, 1994; Takayama *et al.*, 1998; Brown *et al.*, 2017). Furthermore, some of the alkaloids were only found in the Malaysian sample, for instance, mitragynaline, 3,4,5,6-tetrahydromitragynine, mitralactonal and mitrasulgyne (Takayama *et al.*, 1998; Hassan *et al.*, 2013). On the other hand, the major alkaloid derived from the leaves of the plant grown in the United States at the University of Mississippi is the oxindole-type mitraphylline, instead of mitragynine (Leon *et al.*, 2009; Gogineni *et al.*, 2015). In addition, mitragynine and paynantheine were found abundantly in the mature leaves of ketum, whereas speciogynine (Thai

Table 2.1 Alkaloid profile of *Mitragyna speciosa* Korth.

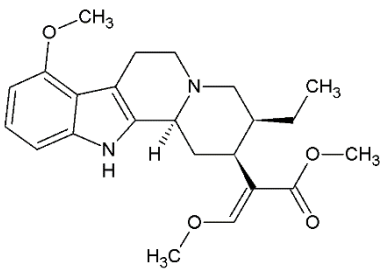
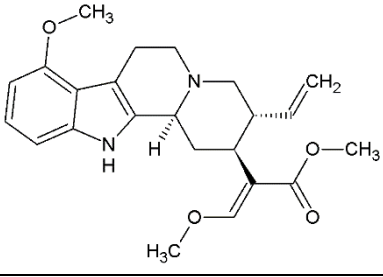
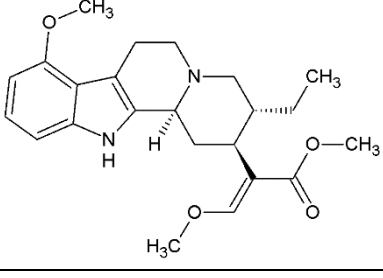
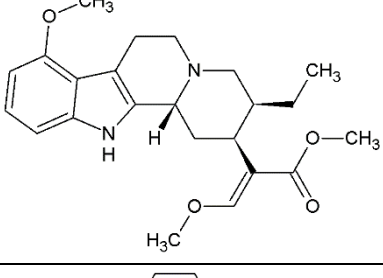
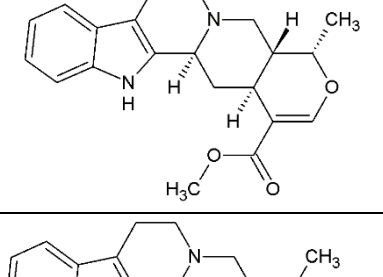
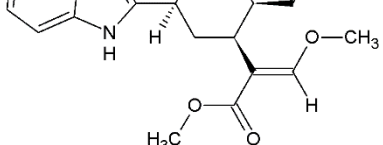
| Alkaloid | Chemical structure | Reference(s) |
|-------------------------|--|--|
| Indole alkaloids | | |
| Mitragynine |  | Beckett <i>et al.</i> , 1966b; Leon <i>et al.</i> , 2009; Ali <i>et al.</i> , 2014; Lesiak <i>et al.</i> , 2014; Wang <i>et al.</i> , 2014; Avula <i>et al.</i> , 2015; Lesiak and Musah, 2016 |
| Paynantheine |  | Beckett <i>et al.</i> , 1966b; Leon <i>et al.</i> , 2009; Ali <i>et al.</i> , 2014; Lesiak <i>et al.</i> , 2014; Wang <i>et al.</i> , 2014; Avula <i>et al.</i> , 2015; Lesiak and Musah, 2016 |
| Speciogynine |  | Beckett <i>et al.</i> , 1966b; Ali <i>et al.</i> , 2014; Lesiak <i>et al.</i> , 2014; Wang <i>et al.</i> , 2014; Avula <i>et al.</i> , 2015 |
| Speciociliatine |  | Beckett <i>et al.</i> , 1966b; Ali <i>et al.</i> , 2014; Lesiak <i>et al.</i> , 2014; Wang <i>et al.</i> , 2014; Avula <i>et al.</i> , 2015 |
| Ajmalicine |  | Beckett <i>et al.</i> , 1966b; Leon <i>et al.</i> , 2009; Lesiak <i>et al.</i> , 2014; Lesiak and Musah, 2016 |
| Corynantheidine |  | Beckett <i>et al.</i> , 1966b; Leon <i>et al.</i> , 2009 |

Table 2.1 Continued

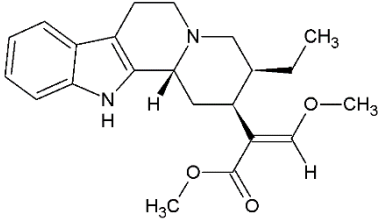
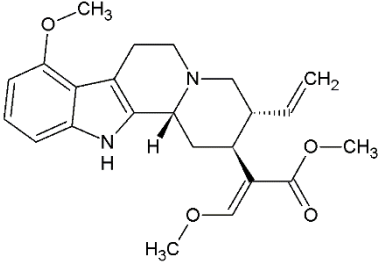
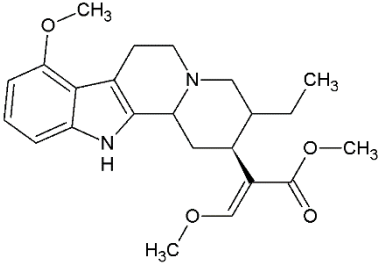
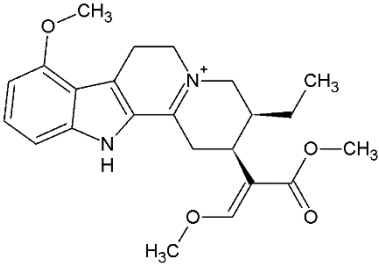
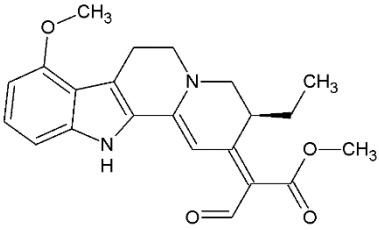
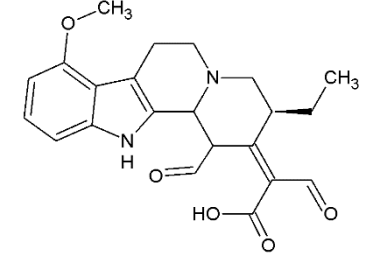
| Alkaloid | Chemical structure | Reference(s) |
|----------------------|--|---|
| Isocorynantheidine |  | Shellard <i>et al.</i> , 1978b; Leon <i>et al.</i> , 2009 |
| 3-isopaynantheine |  | Shellard <i>et al.</i> , 1978b; Ali <i>et al.</i> , 2014; Wang <i>et al.</i> , 2014; Avula <i>et al.</i> , 2015 |
| Mitraciliatine |  | Shellard <i>et al.</i> , 1978b Lesiak <i>et al.</i> , 2014; |
| 3-dehydromitragynine |  | Houghton and Said, 1986 |
| Mitragynaline |  | Houghton <i>et al.</i> , 1991; Takayama <i>et al.</i> , 2001 |
| Mitragynalinic acid |  | Houghton <i>et al.</i> , 1991 |

Table 2.1 Continued

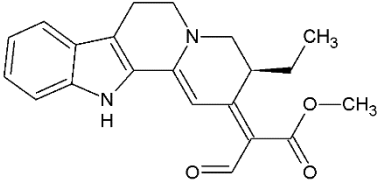
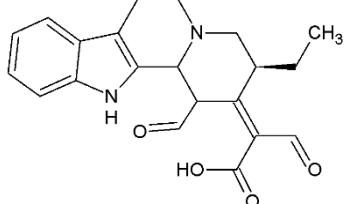
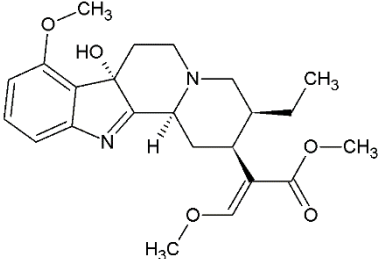
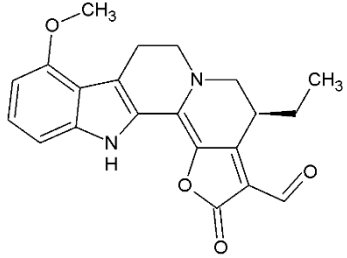
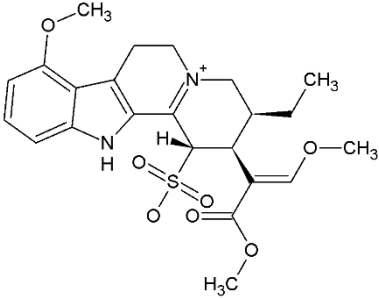
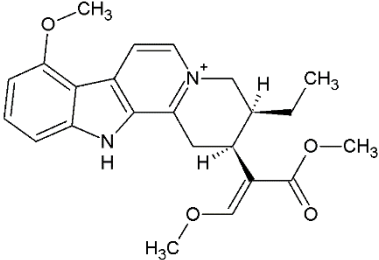
| Alkaloid | Chemical structure | Reference(s) |
|-------------------------------|--|--|
| Corynantheidaline |  | Houghton <i>et al.</i> , 1991; Takayama <i>et al.</i> , 2001 |
| Corynantheidinalinic acid |  | Houghton <i>et al.</i> , 1991 |
| 7-hydroxymitragynine |  | Ponglux <i>et al.</i> , 1994; Leon <i>et al.</i> , 2009; Lesiak <i>et al.</i> , 2014; Avula <i>et al.</i> , 2015; Lesiak and Musah, 2016 |
| Mitrallactonal |  | Takayama <i>et al.</i> , 1998 |
| Mitrasulgynine |  | Takayama <i>et al.</i> , 1998 |
| 3,4,5,6-tetrahydromitragynine |  | Takayama <i>et al.</i> , 1998 |

Table 2.1 Continued

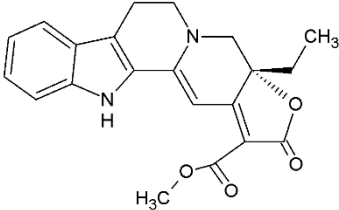
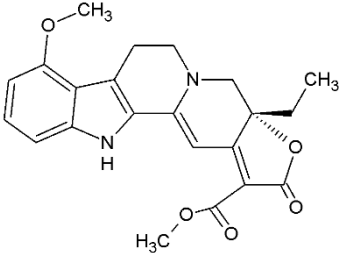
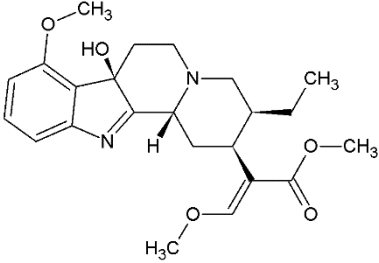
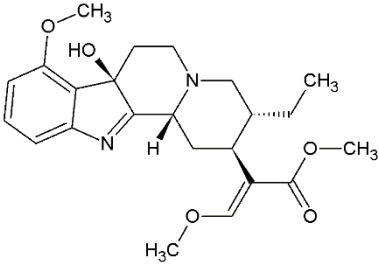
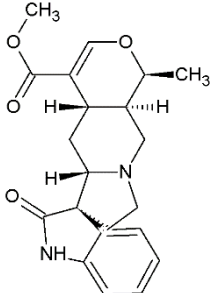
| Alkaloid | Chemical structure | Reference(s) |
|------------------------------|--|--|
| Mitrilactonine |  | Takayama <i>et al.</i> , 1999 |
| 9-methoxymitrilactonine |  | Takayama <i>et al.</i> , 2000 |
| 7-hydroxyspeciociliatine |  | Kitajima <i>et al.</i> , 2006 |
| 7β-hydroxy-7H-mitraciliatine |  | Ali <i>et al.</i> , 2014; Avula <i>et al.</i> , 2015 |
| Oxindole alkaloids | | |
| Mitrephylline |  | Beckett <i>et al.</i> , 1966a; Leon <i>et al.</i> , 2009; Lesiak <i>et al.</i> , 2014; Lesiak and Musah, 2016 |

Table 2.1 Continued

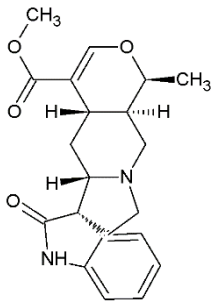
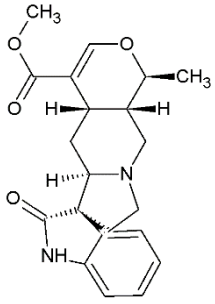
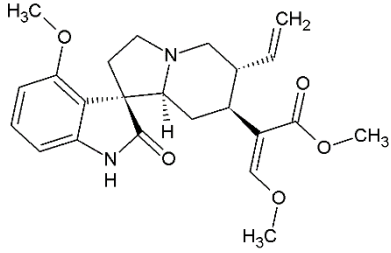
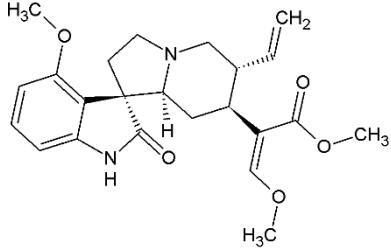
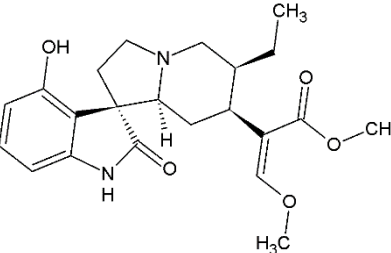
| Alkaloid | Chemical structure | Reference(s) |
|------------------|--|--|
| Isomitraphylline |  | Beckett <i>et al.</i> , 1966a; Leon <i>et al.</i> , 2009 |
| Speciophylline |  | Beckett <i>et al.</i> , 1966a |
| Specionoxeine |  | Trager <i>et al.</i> , 1968; Shellard <i>et al.</i> , 1978b |
| Isospecionoxeine |  | Trager <i>et al.</i> , 1968; Shellard <i>et al.</i> , 1978b |
| Mitrafoline |  | Hemingway <i>et al.</i> , 1975; Shellard <i>et al.</i> , 1978a |

Table 2.1 Continued

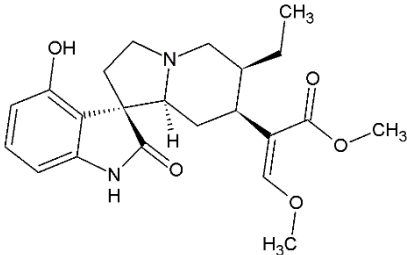
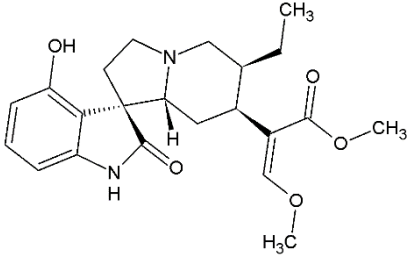
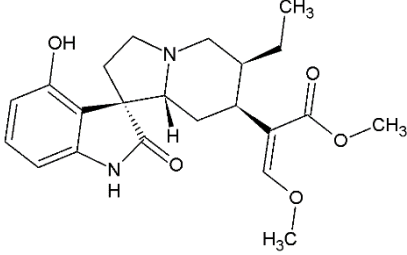
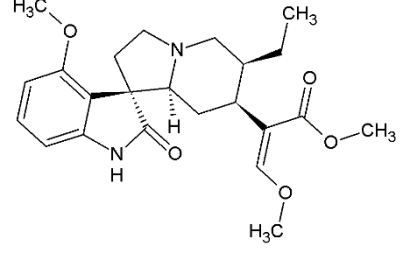
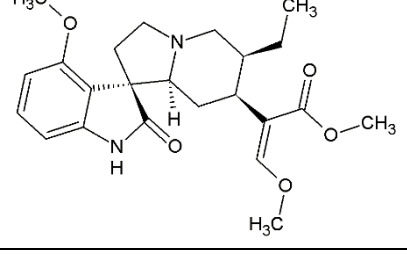
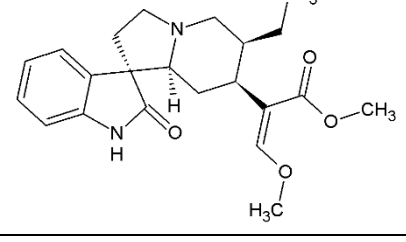
| Alkaloid | Chemical structure | Reference(s) |
|------------------------|--|--|
| Isomitrafoline |  | Hemingway <i>et al.</i> , 1975; Shellard <i>et al.</i> , 1978a |
| Speciofoline |  | Hemingway <i>et al.</i> , 1975; Shellard <i>et al.</i> , 1978a |
| Isospeciofoline |  | Hemingway <i>et al.</i> , 1975; Shellard <i>et al.</i> , 1978a; Ali <i>et al.</i> , 2014; Avula <i>et al.</i> , 2015 |
| Mitragynine oxindole A |  | Shellard <i>et al.</i> , 1978a |
| Mitragynine oxindole B |  | Shellard <i>et al.</i> , 1978a |
| Corynoxine A |  | Shellard <i>et al.</i> , 1978a; Ali <i>et al.</i> , 2014; Wang <i>et al.</i> , 2014; Avula <i>et al.</i> , 2015 |

Table 2.1 Continued

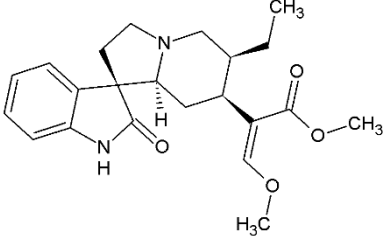
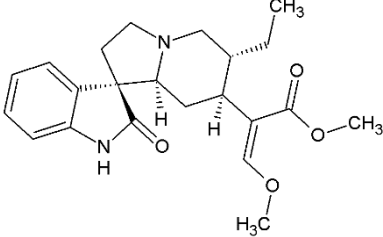
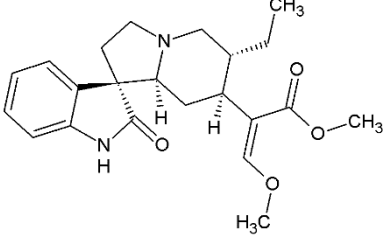
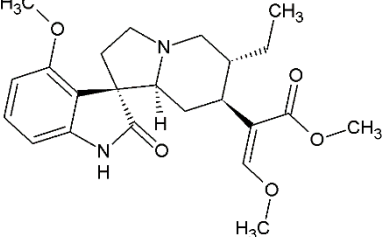
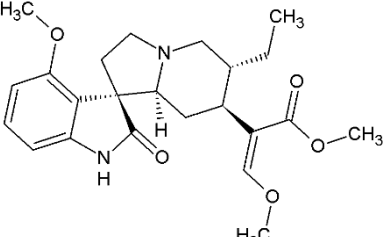
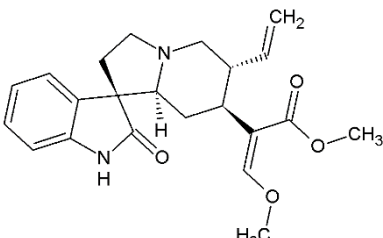
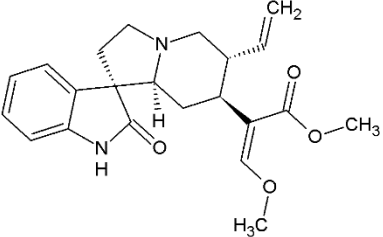
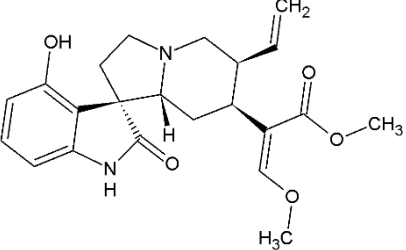
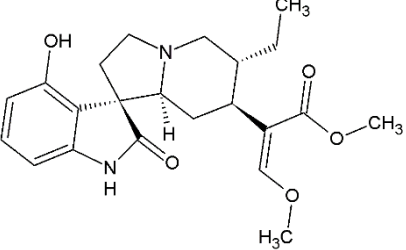
| Alkaloid | Chemical structure | Reference(s) |
|--------------------|--|--|
| Corynoxine B |  | Shellard <i>et al.</i> , 1978a; Ali <i>et al.</i> , 2014; Wang <i>et al.</i> , 2014; Avula <i>et al.</i> , 2015 |
| Rhynchophylline |  | Shellard <i>et al.</i> , 1978a; Lesiak <i>et al.</i> , 2014; Lesiak and Musah, 2016 |
| Isorhynchophylline |  | Shellard <i>et al.</i> , 1978a |
| Rhyncociline |  | Shellard <i>et al.</i> , 1978a |
| Ciliaphylline |  | Shellard <i>et al.</i> , 1978a |
| Corynoxine |  | Shellard <i>et al.</i> , 1978a; Kitajima <i>et al.</i> , 2006; Lesiak <i>et al.</i> , 2014; Lesiak and Musah, 2016 |

Table 2.1 Continued

| Alkaloid | Chemical structure | Reference(s) |
|------------------|--|---|
| Isocorynoxetine |  <p>The chemical structure of Isocorynoxetine features a complex polycyclic core consisting of a benzene ring fused to a five-membered ring containing a nitrogen atom and a carbonyl group. This is further fused to a six-membered ring containing another nitrogen atom. A side chain is attached to the six-membered ring, containing a terminal vinyl group (CH₂), a methyl ester group (COOCH₃), and a methoxy group (OCH₃) on a double bond.</p> | Kitajima <i>et al.</i> , 2006 |
| Isospeciofoline |  <p>The chemical structure of Isospeciofoline is similar to Isocorynoxetine but includes a hydroxyl group (OH) on the benzene ring. The side chain is identical to that of Isocorynoxetine, featuring a vinyl group, a methyl ester, and a methoxy group.</p> | Ali <i>et al.</i> , 2014; Avula <i>et al.</i> , 2015 |
| Isorotundifoline |  <p>The chemical structure of Isorotundifoline is similar to Isospeciofoline but features a methyl group (CH₃) instead of a hydroxyl group on the benzene ring. The side chain remains the same, with a vinyl group, a methyl ester, and a methoxy group.</p> | Ali <i>et al.</i> , 2014; Avula <i>et al.</i> , 2015 |

samples) as well as mitragynaline and corynantheidaline (Malaysian samples) appeared to be the dominant alkaloids in the very young leaves of ketum, suggesting the variation of alkaloid contents in plants of different maturity (Shellard *et al.*, 1978a; Shellard *et al.*, 1978b; Houghton *et al.*, 1991; Brown *et al.*, 2017).

The usage of ketum has gained increasing popularity in the Western countries since the herbal products can be easily accessible over the internet with minimal regulation of their sale (Adkins *et al.*, 2011; Singh *et al.*, 2016). People consume them primarily for recreational purposes, to ease dependence on alcohol, and to cure anxiety and depression (McWhirter and Morris, 2010; Cinosi *et al.*, 2015). Due to the concerns over addiction, possessing or selling ketum leaves or preparations in any form are prohibited in Malaysia, Thailand, Australia and Myanmar, and are listed as controlled drugs in many European Union countries, such as Denmark, Poland and Sweden (Hassan *et al.*, 2013). Despite the tree and its leaves being illegal, there is still a widespread misuse of ketum by the locals in Malaysia and Thailand (Adkins *et al.*, 2011; Singh *et al.*, 2016). In August 2016, the US Drug Enforcement Administration (DEA) announced its plans to list ketum, mitragynine and 7-HMG as controlled substances. However, the plan was temporary put on hold due to public outcry (Prozialeck, 2016). Currently, ketum and ketum-derived drugs are legal in the US, except in certain states like Alabama, Arkansas, Indiana, Tennessee, Vermont and Wisconsin (Prozialeck, 2016). Meanwhile, ketum is legally cultivated in Indonesia and exported on large scale to Asia, Europe and North America, making it harder for the authorities to control the access of ketum (Hassan *et al.*, 2013).

In spite of the wide range of pharmacological effects, reports of toxicity related to ketum use are scarce. Most of the *in vivo* studies involved the acute oral toxicity of ketum extracts in animal models. In addition, clinical toxicological investigations were

limited to a few human case-reports concerning the toxic effect of ketum extracts following short or long term consumption (Sabetghadam *et al.*, 2013a). Ketum and its related products have been linked to severe drug toxicity. Cases of ketum use associated with seizures have been reported after co-administering the herb with modafinil (Boyer *et al.*, 2008) and *Datura stramonium* (Nelsen *et al.*, 2010). Majority, but not all, of the cases linked to death involved those who had abused other substances along with ketum or had histories of alcohol dependence or heroin abuse (Singh *et al.*, 2016). Ketum has been shown to cause serious adverse effects, such as elevated blood pressure, nephrotoxic effects, impaired cognition and behavior, dependence potential, and hepatic failure (Apryani *et al.*, 2010; Harizal *et al.*, 2010; Kapp *et al.*, 2011; Cinosi *et al.*, 2015; Yusoff *et al.*, 2016). However, the cardiac toxicity of ketum and its analogues is not clearly known (Lu *et al.*, 2014).

Lu and co-workers (2014) reported an *in vitro* cardiac toxicity study of mitragynine and its analogues using recombinant HEK293 cell expressing human ether-a-go-go-related gene 1a channel (HEK293-hERG1a) and human induced pluripotent stem cell-derived cardiomyocytes (hiPSC-CMs). They found that 10 μM mitragynine significantly reduced the rapid outward delayed rectifier potassium current (I_{Kr}) current in HEK293-hERG1a. In addition, mitragynine, paynantheine, speciogynine and speciociliatine dosage-dependently (0.1 – 100 μM) suppressed I_{Kr} in hiPSC-CMs by 67% - 84% with IC_{50} values ranging from 0.91 to 2.47 μM . Furthermore, mitragynine at 10 μM was found to significantly prolong the action potential duration (APD) at 50 and 90% repolarization respectively (APD50 and APD90). They concluded that these alkaloids may trigger TdP via inhibition of I_{Kr} in human cardiomyocytes (Lu *et al.*, 2014). Nevertheless, the effects of mitragynine on channel trafficking remained unknown. Apart from acute hERG1 inhibition via

channel blockade, hERG1 channel trafficking defect represents the alternative yet more chronic cellular mechanism of hERG1 inhibition (Steele *et al.*, 2007; Nogawa and Kawai, 2014).

2.2 The cardiac action potential

A body surface electrocardiogram (ECG) demonstrates the electrophysiological events taking place during impulse generation and conduction in the heart. Each heartbeat starts as an electrical stimulus generated in the sinoatrial (SA) node and is rapidly spreading out through the atria. The impulse from the SA node eventually passes through the atrioventricular (AV) node and rapidly propagates to both ventricles via the His-Purkinje system. The 'P' wave on the ECG measurement reflects the combined electrical activity of action potential depolarization in the atria. The QRS complex represents the action potential depolarization occurring in the ventricles, whereas the T wave corresponds to the ventricular repolarization. Hence, the QT interval of an ECG, which is measured in milliseconds (ms), demonstrates the duration of the ventricular depolarization and repolarization, plus the time associated with transmission across the cardiac muscles (Figure 2.1) (Finlayson *et al.*, 2004; Amin *et al.*, 2010; Qu *et al.*, 2014).

The generation of cardiac action potential is contributed by the selective permeability of ion channels distributed on the cardiomyocytes membrane, as shown in Figure 2.2. The inward depolarizing currents, primarily through Na^+ and Ca^{2+} channels, contribute to normal depolarization, whereas outward repolarizing currents, predominantly through K^+ channels, result in repolarization (van Noord *et al.*, 2010). The human ventricular action potential consists of five sequential phases (phases 0 to 4). Initially, the cell is polarized near to the equilibrium potential for potassium ions

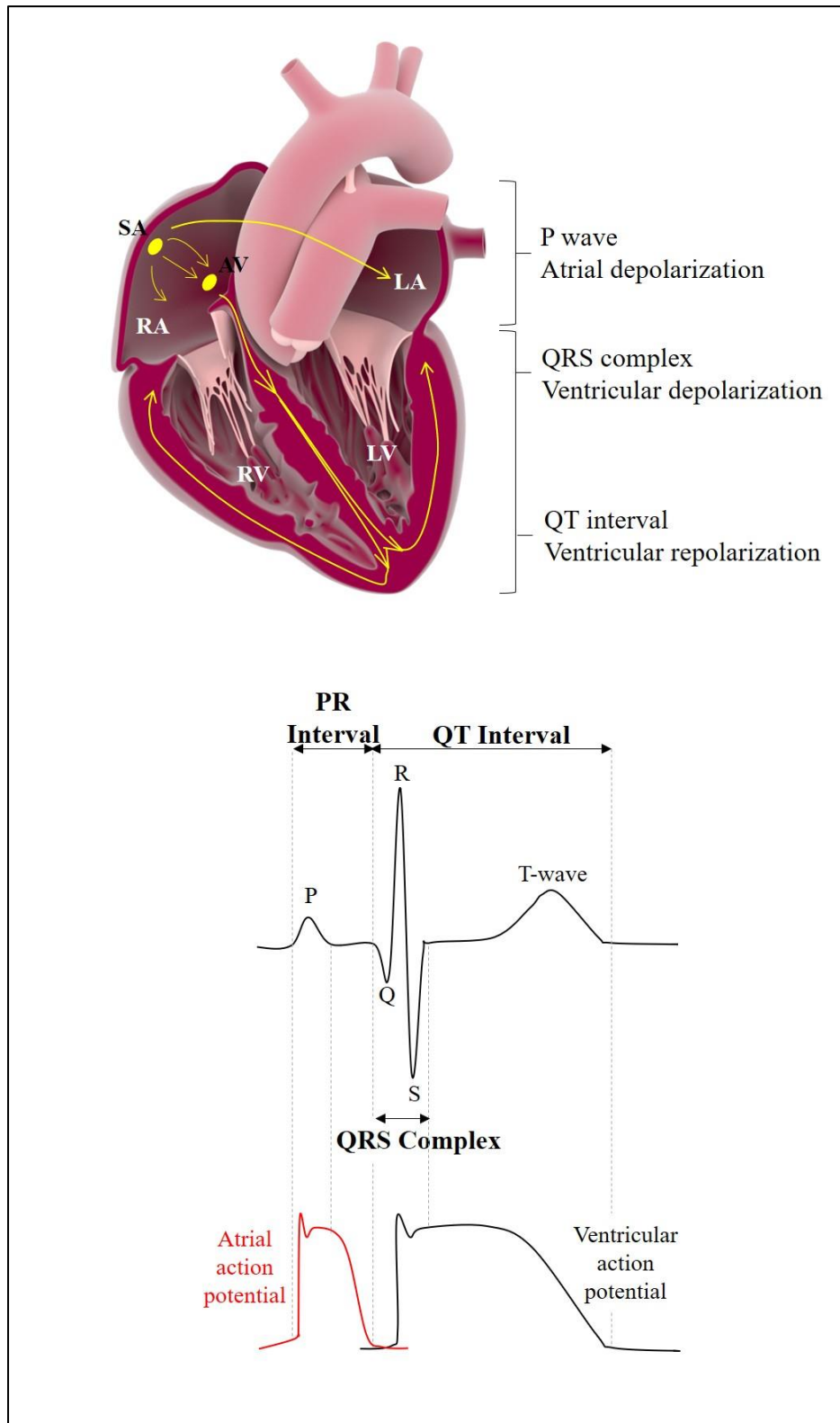


Figure 2.1 The electrical activity of the heart presented on the surface electrocardiogram (ECG). The ‘P’ wave reflects the combined electrical activity of action potential depolarization in the atria. The QRS complex represents the action potential depolarization in the ventricles, whereas the T wave corresponds to the ventricular repolarization. (Adapted from Amin *et al.*, 2010 and Qu *et al.*, 2014)

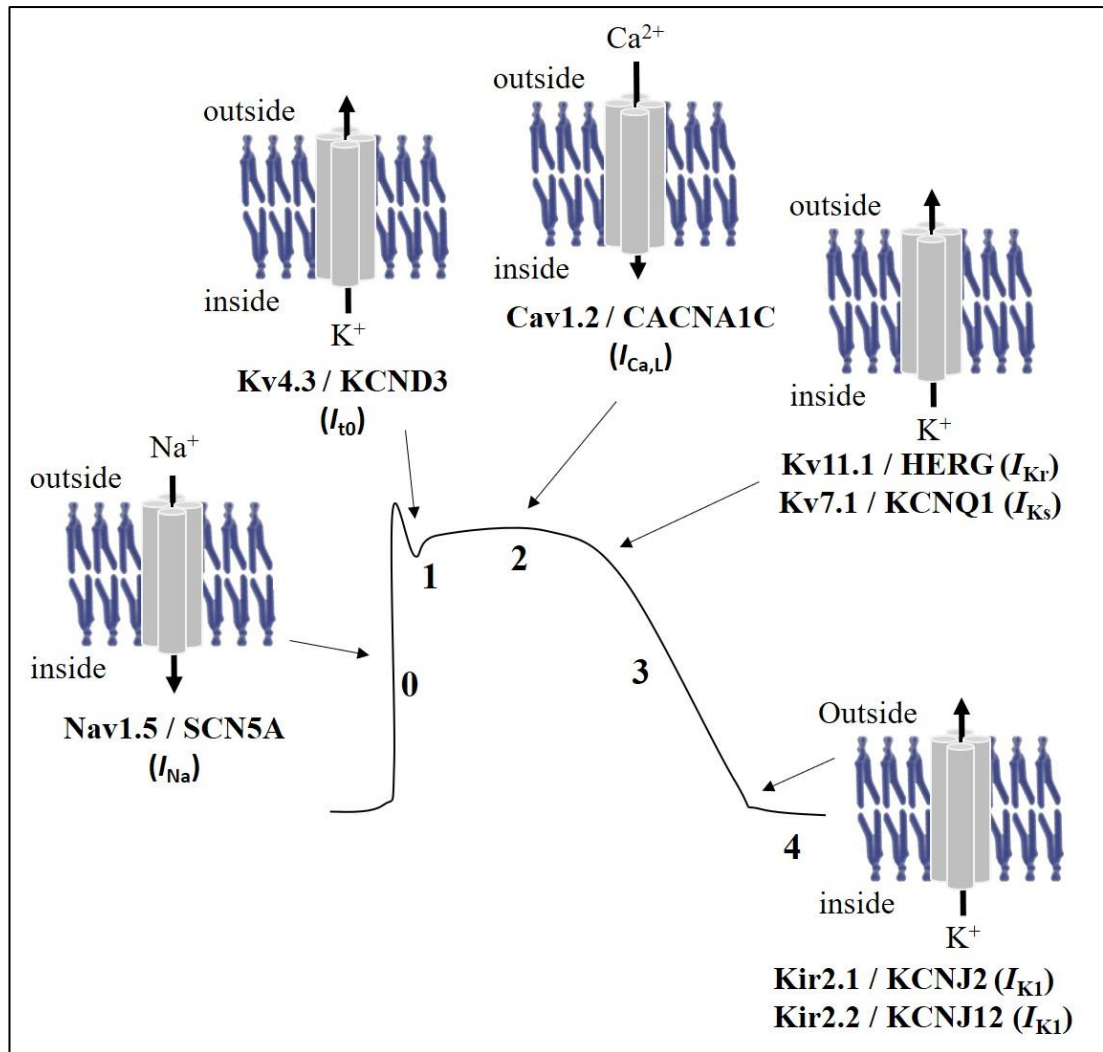


Figure 2.2 The ventricular cardiac action potential and cardiac ion channels. The upstroke (phase 0) is triggered by the large inward Na^+ current (I_{Na}). The rest of the action potential (phase 1 to 4) is controlled by the interplay of depolarizing Ca^{2+} channels (mainly Cav1.2) and repolarizing K^+ channels that regulate the transient outward current (I_{to}), the rapid and slow delayed rectifiers currents (I_{Kr} and I_{Ks}) and the inward rectifier current (I_{K1}). (Adapted from Pollard *et al.*, 2010 and George, 2013)

(E_K) due to the high K^+ conductance at rest (phase 4). A rapid depolarization of the membrane (phase 0) is triggered by the large inward Na^+ current. Repolarization is much slower and occurs in three phases. A brief partial repolarization, which lasts only a few milliseconds, follows rapidly (phase 1); this is caused by inactivation of fast Na^+ channels and a transient outward current (I_{t0}), comprising of two components, one a Cl^- current, and the other by a K^+ current. A much slower rate of repolarization, known as the plateau phase (phase 2), of the action potential then follows; this is a dynamic equilibrium between inward movement of Ca^{2+} through L-type calcium channels and outward movement of K^+ . The plateau phase delays the cardiac action potential duration because the K^+ channels that repolarize the membrane either activate slowly, inactivate rapidly, or conduct less current at positive transmembrane potentials. A long action potential allows sufficient time for influx of extracellular Ca^{2+} for optimum excitation-contraction coupling and also renders the cardiomyocytes comparatively refractory to premature excitation. Subsequently, the cell membrane slowly repolarizes when K^+ efflux exceeds Ca^{2+} influx. This repolarization (phase 3) increases the conductance of some K^+ channels while reduces the Ca^{2+} current, resulting in a net outward positive current. The augmenting K^+ current rapidly induces complete repolarization and returns the membrane potential of the cardiac muscle cells to its original resting level (Finlayson *et al.*, 2004; Sanguinetti and Tristani-Firouzi, 2006; Zünkler, 2006; Pollard *et al.*, 2010; George, 2013).

There are three major K^+ currents involving in the repolarization of ventricular myocytes action potential, namely the transient outward K^+ current (I_{t0}), the delayed rectifier K^+ current (I_K) and the inward rectifier K^+ currents (I_{K1}). I_{t0} contributes to the phase 1 repolarization of the action potential, whereas I_{K1} maintains the resting membrane potential and leads to the late repolarization phase (Zünkler, 2006; Hancox

et al., 2008; Jeevaratnam *et al.*, 2017). I_K is the major outward current that is responsible in mediating cardiac action potential repolarization, and thus, is crucial in determining the duration of the action potential. Noble and Tsien (1969) first provided evidence for two kinetically distinct components of the I_K in cardiac myocytes, which they named I_{K1} and I_{K2} (Noble and Tsien, 1969). In 1990, Sanguinetti and Jurkiewicz demonstrated that the two components differed in pharmacological sensitivity, in which certain class III antiarrhythmic drugs selectively blocked the rapid component, which they named I_{Kr} , whereas the slow component, I_{Ks} was highly sensitive to activation by β -adrenergic stimulation (Sanguinetti and Jurkiewicz, 1990). Subsequently, the presence of both components was proven in human ventricular myocytes (Li *et al.*, 1996; Grant, 2009; Jeevaratnam *et al.*, 2017).

2.3 Long QT syndrome (LQTS)

Long QT syndrome (LQTS) is a disorder portrayed by delayed ventricular myocyte repolarization, which is illustrated by abnormal prolongation of the QT interval on the body surface ECG (Figure 2.3) (van Noord *et al.*, 2010; Barsheshet *et al.*, 2014; Gintant *et al.*, 2016). The QT interval is influenced by heart rate and hence the QT interval is normally corrected for heart rate (QTc). Apart from that, the normal and lengthened QTc values rely on gender and age. The American Heart Association, the American College of Cardiology Foundation and the Heart Rhythm Society (AHA/ACCF/HRS) Recommendations for the Standardization and Interpretation of the Electrocardiogram recommended that the QTc greater than 450 ms and 460 ms in adult males and adult females, respectively, be regarded as a prolonged QT interval, whereas QTc shorter than 390 ms be considered a short QT interval (Rautaharju *et al.*, 2009; Postema and Wilde, 2014). Patients with QTc greater than 500 ms are

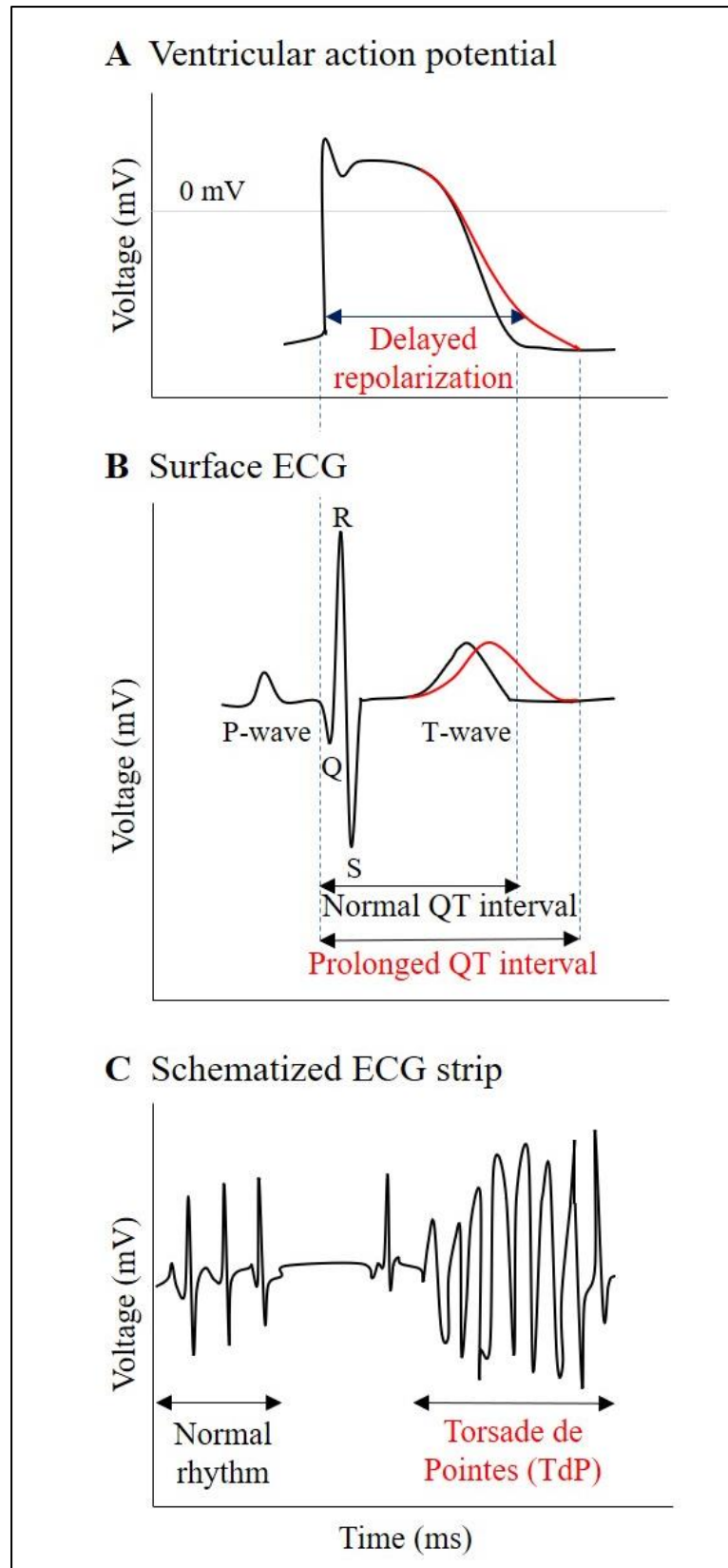


Figure 2.3 Relationship between (A) delayed repolarization, (B) prolonged QT interval and (C) Torsade de Pointes (TdP) cardiac-arrhythmia (Adapted from Gintant *et al.*, 2016).

predisposed to a ventricular tachyarrhythmia, specifically Torsade de Pointes (TdP), characterized by continuously twisting of the QRS complexes around the isoelectric line of the ECG, which either spontaneously terminates or degenerates into ventricular fibrillation, leading to syncope and sudden death (Postema and Wilde, 2014).

2.3.1 Congenital LQTS

Congenital LQTS is an inherited form of LQTS affecting young otherwise healthy individuals and is related to recurrent spontaneous syncope, which often results in cardiac arrest and sudden cardiac death due to ventricular tachyarrhythmia and fibrillation. The estimated prevalence of LQTS is about 1 in 2,500 live births (Finlayson *et al.*, 2004; Crotti *et al.*, 2008; van Noord *et al.*, 2010; Barsheshet *et al.*, 2014).

The first incidence of congenital LQTS may have been depicted by Meissner in Germany in 1856 (Meissner, 1856). He described a deaf girl who collapsed and died while being reprimanded at school. The girl had two brothers who also died suddenly after a severe fright or intense fury. This report preceded the development of ECG and thus the QT intervals of this family were not interpreted (Meissner, 1856; Vincent, 2002; Finlayson *et al.*, 2004). It was more than a century later when Jervell and Lange-Nielsen (1957) presented the electrocardiographic basis for LQTS. In a family with six siblings, four were deaf and suffered repeated syncope during exercise or without apparent cause. Three of them died suddenly, at the ages of 4, 5 and 9 years respectively. Electrocardiographic studies in three of the cases demonstrated a distinct QT interval prolongation. No apparent abnormality of the heart was observed (Jervell and Lange-Nielsen, 1957; Vincent, 2002; Finlayson *et al.*, 2004). Thereafter, Romano and Ward reported families with a cardiac abnormality almost identical to that described by Jervell and Lange-Nielsen but with normal hearing, suggesting a similar